Catalysis Today 144 (2009) 341–349

Contents lists available at ScienceDirect

Catalysis Today

journal homepage: www.elsevier.com/locate/cattod

Autothermal reforming of diesel fuel in a structured porous metal catalyst: Both kinetically and transport controlled reaction

Alexey B. Shigarov *, Victor V. Kireenkov, Valery A. Kuzmin, Nikolay A. Kuzin, Valery A. Kirillov

Boreskov Institute of Catalysis, Prosp. Akad. Lavrentieva 5, 630090 Novosibirsk, Russia

ARTICLE INFO

Article history:
Available online 13 March 2009

Keywords:
Autothermal reforming
n-Decane
Diesel fuel
Structured metal porous catalysts
Mathematical modeling
Kinetically and transport controlled reactions

ABSTRACT

Autothermal reforming (ATR) of diesel fuel into syngas was studied experimentally and theoretically. The experiments were performed in a reactor consisting of two cylindrically shaped monoliths 50 × 55 mm. Different catalytically active components and supports (Co, Mn, Rh, BaO, La_2O_3/Al_2O_3 and SiO_2) were tested. The reactor parameters were as follows: $O_2/C = 0.5$, $S/C = 1.5–1.7$, $T_{in} = 350–400$ °C. The regularly structured catalytic monoliths were prepared using various metal porous supports. The most active and coke resistant catalyst was determined. The original modeling approach was based on the assumption that ATR involves two parallel reaction routes: (1) complete hydrocarbon oxidation, (2) steam reforming of hydrocarbon. The experimental data and the results of reactor modeling agreed well and allowed a conclusion that the ATR rate is controlled by inter-phase mass transfer. However, the contribution of the reaction routes (1) and (2), i.e., the distribution of hydrocarbon flux between these reactions is determined by the ratio of the reaction rate constants and oxygen concentration near the surface.

1. Introduction

During the past decade, on-board production of hydrogen from traditional fuels (natural gas, gasoline, diesel) has become the focus of intensive research investigations both in catalytic and engineering aspects. Small scale fuel processors (1–100 kW) are promising for fuel cell and deNO_x systems in transportation and portable power applications. A brief review of possible approaches to this problem made in [1] points out the advantageous position of autothermal reforming (ATR) among two other possibilities (steam reforming, partial oxidation) because the ATR-reactor rapidly responses to changing power demand, startups faster and operates at lower temperature, which allows a less complicated reactor design, wider choice of materials and lower fuel consumption during start-up.

Despite all the mentioned attractive features, ATR of diesel fuel presents an additional problem to a process designer because the boiling point of the most diesel components (higher hydrocarbons) is higher than the ignition point. Surprisingly, only few experimental and absolutely no modeling efforts concerning diesel ATR are available in open literature. One of the reasons is that diesel fuel is a complex mixture of different hydrocarbons ($C_8–C_{20}$) that significantly complicates experimental and theoretical studies of its catalytic reforming into synthesis-gas. Indeed, no commonly agreed concept of a possible reaction scheme for autothermal reforming of higher hydrocarbons is still available. Authors [1] suggest a scheme based on the complete hydrocarbon oxidation to CO_2 and H_2:

$$C_nH_m + xO_2 + (2n-2x)H_2O = nCO_2 + (2n-2x+m/2)H_2. \quad (1)$$

However, this equation does not take into account the presence of methane in the reaction products, which was experimentally observed in a number of experimental works [2–5]. Another scheme of the diesel autothermal reforming is suggested in [6]:

$$C_nH_m + nH_2O = nCO + (n+m/2)H_2, \quad (2)$$

$$C_nH_m + n/2O_2 = nCO + m/2H_2, \quad (3)$$

$$CO + H_2O \rightarrow CO_2 + H_2, \quad (4)$$

$$CO + 3H_2 \rightarrow CH_4 + H_2O. \quad (5)$$

This scheme explains the appearance of methane in the reactions products, but according to [4], methanation reaction (5) is thermodynamically unfavorable under autothermal reforming conditions. The authors of [4] suggest additional reaction route:

$$C_nH_m \rightarrow CH_4 + C_{n-1}H_{m-4} \quad (6)$$

* Corresponding author.
E-mail address: shigarov@catalysis.ru (A.B. Shigarov).

0920-5861/$ – see front matter © 2009 Elsevier B.V. All rights reserved.
doi:10.1016/j.cattod.2009.01.043

Nomenclature

c_p specific heat capacity of gas (J/(kg K))
$d = 0.003$ m diameter of channels in the structured catalyst bed
$D_{HC} = 1.8 \times 10^{-5}$ m^2/s diffusion coefficient of *n*-decane vapor in the gas mixture (at 350 °C)
$D_{O_2} = 7.9 \times 10^{-5}$ m^2/s diffusion coefficient of oxygen in the gas mixture (at 350 °C)
E_{ox}, E_{ref} energy of activation of complete oxidation and steam reforming of *n*-decane (J/mol)
G mass velocity of gas (kg/(m^2 s))
j_{HC}, j_{O_2} mole fluxes of *n*-decane and oxygen across a gas–solid interface (mol/(m^2 s))
$\Delta H_{ox} = 6.35 \times 10^6$ J/mol ($C_{10}H_{22}$) heat effect of the reaction of complete oxidation of *n*-decane (at 350 °C)
$\Delta H_{ref} = 1.64 \times 10^6$ J/mol ($C_{10}H_{22}$) heat effect of the reaction of steam reforming of *n*-decane (at 350 °C)
k_{ox}, k_{ref} rate constants of the complete oxidation and steam reforming reactions of *n*-decane, mol $C_{10}H_{22}$/(m^2 s)
ℓ coordinate along the reactor length (m)
L reactor length (m)
m_i mole mass (kg/mol)
Q_{air}, Q_{H_2O}, Q_{HC} flow rates of air, water and hydrocarbon (*n*-decane)
$R = 8.31$ J/(mol K) the constant of ideal gas
$S = 1200$ m^{-1} specific geometric surface of the catalyst bed
$Sh = Nu = 2.7$ Sherwood and Nusselt numbers for stabilized flow in a triangular channel
T_S, T_g temperature of catalyst and gas
W_{ox}, W_{ref} apparent reaction rates of complete oxidation, steam reforming of *n*-decane (mol/(m^{2}s))
x_i mole fractions of gas components in a flow
x_i^s mole fractions of gas components on the catalyst surface
y_i mass fractions of gas components in a flow

Greek letters
α coefficient of gas-solid heat transfer (W/(m^2 K))
β_{HC}, β_{O_2} coefficients of gas-solid mass transfer for *n*-decane and oxygen (m/s)
φ_{ox}, φ_{ref} fractions of *n*-decane total diffusion flux (from gas to the catalyst surface) consumed by reactions of complete oxidation and steam reforming.
$\lambda = 0.06$ W/(m K) coefficient of heat conductivity of the gas mixture (at 350 °C)
ρ molar density of the gas mixture (at 350 °C) (mol/m^3)

Subscripts
g gas phase
HC hydrocarbon (*n*-decane)
i = HC, O_2, H_2O, CO, CO_2, H_2, N_2 components of gas mixture
ox complete oxidation of *n*-decane
ref steam reforming of *n*-decane.
S catalyst surface

Further progress of the reaction occurs due to reforming of $C_{n-1}H_{m-4}$ into H_2, CO, CO_2 and residual hydrocarbons. Although this scheme explains the appearance of methane in the reaction products, it is not verified experimentally. The lack of appropriate reaction schemes for diesel fuel autothermal reforming facilitated the studies of ATR of individual hydrocarbons as diesel fuel simulators. Decane, decalin, tetradecane were used as the diesel fuel models [4,5]. Regarding the rates of synthesis gas generation over a platinum catalyst, the authors of [4] arranged the studied hydrocarbons in the following order:

Aromatics≪naphthenes<paraffins.

It was also established that at short contact times (GHSV = 50,000–100,000 h^{-1}) and low temperatures, the reaction products contain aldehydes, ketones, cracking products, aromatics dehydration products, etc. The yields of hydrogen and CO increased with increasing temperature and contact time that indicates further reforming of all intermediate products into resulting products. The maximal hydrogen yield was achieved at GHSV = 2000–10,000 h^{-1} and T = 840–880 °C [5]. Paper [7] reports the effect of the process parameters on the yield of hydrogen. The effect of S/C = 1–3 on the hydrogen content in the reaction products was insignificant. Increasing S/C suppressed carbon formation but decreased the overall efficiency. The maximum hydrogen yield was obtained at O/C = 0.7–1.2. Note that it was strongly dependent on the type of converted hydrocarbon. However, these data contradict the results reported in [8]. Here, the authors made an attempt to derive a kinetic equation for apparent reaction rate. They observed the first order reaction rate with respect to water and approximately zero order with respect to oxygen.

In addition, the diesel autothermal reforming catalysts should provide stable operation during at least 1000 h, and appropriate sulfur and coke resistance. That is, most researchers used platinum group metals such as Rh, Pt, Pd or perovskite-like metal oxides ($LaCrO_3$, $LaMnO_3$, $LaFeO_3$, $LaCoO_3$, $LaNiO_3$) in their investigations. To improve sulfur resistance and activity, the studied catalyst were doped with gadolinium and cerium oxides. In the autothermal gasoline reforming [3,9], Rh and Rh-Pt doped with Gd and CeO_2 provided the yield of 8.7 and 9.3 mol of hydrogen per 1 mol of hydrocarbon at 700–750 °C. Under similar conditions, the platinum based catalysts provided 2.5 mol of hydrogen. Note that the yield of methane was 0.4 mol per 1 mol of gasoline. Addition of sulfur complexes (30–50 ppm) considerably reduced the catalyst activity. As the reaction temperature rises to 800 °C, the effect of sulfur significantly decreases, especially for catalyst Rh/Al_2O_3. The authors mentioned also a strong effect of the support on the hydrogen yield. Thus, catalyst Rh/Al_2O_3 provided 12 mol of hydrogen per 1 mol of gasoline, catalyst Rh/CeO_2 provided 7 mol of hydrogen per 1 mol of gasoline, and perovskite catalysts yielded 8 mol of hydrogen per 1 mol of gasoline. Paper [10] summarizes the results of ATR (followed by WGS and PROX) of iso-octane-based fuel in a Microlith short-contact time reactor with Pt-Al and Rh-CeZr catalysts. Very important measurements of catalyst temperature and gas mixture composition at six points along the reactor length were reported. The same research group shortly reports in [11] on a fuel processor based on ATR of a diesel, Jet-A or JP-8 logistic fuels with quite promising durability tests. The partial oxidation of *n*-decane and *n*-hexadecane over Rh-coated monoliths (ceramic foams) at contact times 5–25 ms under varying C/O = 0.4–3 ratio was investigated in [12]. Mostly olefins were produced beyond the syngas ratio C/O > 1. In the following paper [13], hydrocarbon mixtures (*n*-octane + i-octane, *n*-decane + *n*-hexadecane, *n*-decane + naphthalene) were partially oxidized over the same catalyst. It was found that the overall reactivity of these mixtures is not simply an average over the reactivities of constituent

molecules. Recently, the same research team shifted their efforts from partial oxidation to ATR of *n*-decane, n-hexadecane and JP-8 military fuel [14] and found that steam addition significantly suppressed olefins production and reduced catalyst coking. Unfortunately, experimental setup did not allow authors [12–14] to measure catalyst temperature at the monolith inlet (only at the outlet), where hot spot formation is possible. Besides, no modeling attempts were made in all of the mentioned studies in order to characterize these processes quantitatively.

In our early paper [15], methane partial oxidation over metal porous structured Ni-catalyst was studied both experimentally and via modeling. Essential progress in making bridges between experiment and theory was based on the accurate measurement of catalyst temperature profile and successful choice of reaction scheme. Shortly speaking, the lumped kinetic parameters for methane POX were derived from experimental data on the catalyst temperature profile and outlet concentrations. It seems reasonable to employ the main principles of that approach for the studies of diesel fuel ATR.

Therefore, the first task of this research was to develop active, coke resistant, structured catalyst for diesel fuel ATR into syngas with $H_2/CO > 3$. The second task was to develop a mathematical model with lumped kinetic parameters and perform a comparative analysis of experimental and calculated data in order to gain some insight in diesel ATR features. One of intriguing aspects (both in academic and practical meanings) concerns the following question: is the reaction kinetically or transport controlled?

2. Experimental

2.1. Reactor, setup and procedure

The scheme of diesel fuel autothermal reformer is shown in Fig. 1. The reactor has a coaxial design, in which the axial-type regular structured (monolith) catalyst is placed. The reactor is made of a heat-insulated stainless steel tube with a flange (the inner tube diameter is 74 mm, the tube length is 70 mm). To provide heat recuperation, an exhaust gas flow was directed into a space between the external and internal tubes, a catalyst monolith is separated from the shell by two shields (to prevent heat losses). The shell (tube of 84 mm in diameter and 160 mm in length) is supplied with a flange to which the flange of internal tube is joined. K-type thermocouples (1.5 mm in diameter) were used for a temperature profile measurement of the reformer in four points: gas mixture inlet T_1, first catalyst monolith entrance T_2, space between the first and second catalyst monoliths T_3 and at reformer outlet T_4. For evaporation of a mixture of diesel fuel and water, a new counter-current evaporator with enlarged evaporation surface and controlled heating power was developed and manufactured. The evaporator represents a tubular reactor in which diesel fuel and water mixture was injected by means of a nozzle in the needed ratio. For heat supply, a part of synthesis gas was oxidized in a separate reactor and counter currently fed into the evaporator. To provide effective evaporation of the diesel fuel-water mixture in the catalyst bed, the mixture was sprayed by means of a pneumatic nozzle. Fig. 2 shows a schematic of the setup for diesel fuel ATR catalyst testing. The setup contains the following parts: a catalytic burner, an evaporator of diesel fuel (a mixture of heavy hydrocarbons) and water, autothermal reformer, feeding and control systems, and analytical equipment. The system of feed preparation comprises control devices (gas and liquid mass flow meters) and an evaporator. Diesel fuel with extremely low concentration of sulfur (≤0.0021%) generated by Achinsk refinery "East Oil Company" was used in all runs (see Table 1 for details).

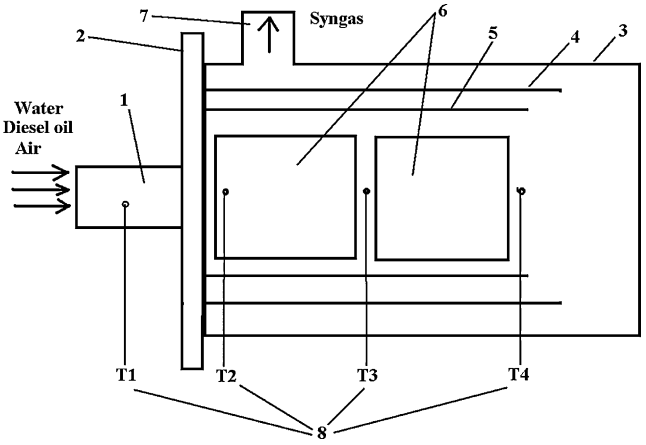

Fig. 1. Schematic diagram of the autothermal diesel fuel reformer and location of thermocouples: (1) inlet fitting into reactor, (2) flange, (3) shell, (4) shields, (5) inner tube, (6) catalytic monoliths, (7) outlet fitting, (8) location of thermocouples in the reactor.

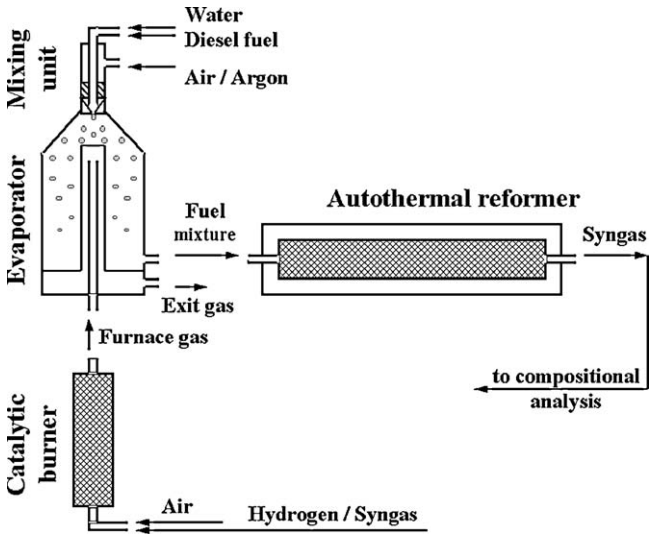

Fig. 2. Scheme of the setup for diesel fuel ATR catalyst tests.

2.2. Start-up and shutdown

The start-up was initiated with feeding of air and hydrogen into the tubular catalytic reactor. The evaporator was heated by means of exhaust gases. As the temperature in the reformer achieved 400 °C, the hydrogen flow was changed by a mixture of diesel fuel and water. The air-vapor mixture heated to 320 °C was directed into the autothermal reformer. For the reactor shutdown, the air supply was cut off first, then the fuel and water feed were turned off. Finally, air was fed on the hot catalyst to burn-off carbon deposited on the surface.

Table 1
Characteristics of the tested diesel fuel.

No.	Characteristic name	Actual value
1	Cetane number	52
2	Viscosity at 20 °C (mm^2/s)	4.94
3	Fractional composition: 50% evaporated at (°C)	214
4	Fractional composition: 96% evaporated at (°C)	258
5	Sulfur concentration (mg/kg)	21
6	C (wt.%)	86.8
7	H (wt.%)	13.68
8	Total content of aromatics in diesel fuel (wt.%)	6.86
9	Fuel formula	$CH_{1.89}$

2.3. Catalysts for autothermal reforming of diesel fuel into synthesis gas

Specific operation conditions of on-board diesel fuel reformer formulate new requirements to catalyst properties, development and applications. The top requirements are: high thermal stability and oxidation resistance of the support; 1–5 W/m K thermal conductivity of a catalyst layer; catalyst life not less than 6000 h; feasibility to use catalyst as a constructional element of the reactor; low cost; similar thermal expansion coefficients of the support and catalytically active layer; good adhesion of the catalyst layer and the metal surface. Based on the earlier tests, we concluded that the catalysts supported on the structured gauze exhibiting sufficiently high longitudinal and radial heat conductivity can serve as a basis for the catalyst development. The preparation technology of monolith reinforced metal porous catalysts for synthesis gas generation from natural gas [15] has recently been developed at the Boreskov Institute of Catalysis. Exactly this technology was used to prepare a catalyst for diesel fuel ATR. The following catalyst samples were prepared:

- *A1*: A porous metal monolith catalyst supported on stainless steel gauze (91.5% of total catalyst weight), covered by 1.5% Al_2O_3 and SiO_2 (1:1) and containing Co and Mn (7 wt.%, Co/Mn = 4.6/6.5) as the active components.
- *A2*: A porous metal monolith catalyst supported on stainless steel twill-weaved gauze (91.6% of the total catalyst weight), containing a mixture of BaO and MnO_2 (5.74% of the total catalyst weight, Ba/Mn = 5/4), and calcined at 650 °C. The as-prepared support was impregnated with Co_3O_4 (2.63% of the total catalyst weight) and calcined at 650 °C.
- *A3*: A porous metal monolith catalyst made of a Fechral gauze (78.8% of the total catalyst weight) covered with a mixture of BaO and MnO_2 (12.16% of the total catalyst weight, Ba/Mn = 5/4), and calcined at 650 °C. The as-prepared reinforced support was impregnated with Co_3O_4 (9.06% of the total catalyst weight) and thermally treated at 650 °C.
- *A4*: A porous metal monolith catalyst based on the stainless steel twill-weaved gauze (90.7% of the total catalyst weight), with a mixture of BaO and MnO_2 (6.98% of the total catalyst weight, Ba/Mn = 5/4) supported on the gauze to increase its surface. Further calcination was performed at 650 °C. The as-prepared reinforced support was impregnated with Co_3O_4 (2.27% of the total catalyst weight) and calcined at 650 °C.
- *A5*: A porous metal monolith catalyst based on the stainless steel twill-weaved gauze. The as-prepared reinforced support was impregnated with salts of Rh (7% of the total catalyst weight) and thermally treated at 650 °C.
- *A6*: A porous metal monolith catalyst based on the stainless steel twill-weaved gauze covered with γ-Al_2O_3 (10% of the monolith weight) and heated at 450 °C. The resulting composite was impregnated with solutions of potassium carbonate (K_2O = 1%) and solutions of lanthanum and barium nitrates (BaO = 2.5%, La_2O_3 = 10%). The as-prepared reinforced support was impregnated with nickel nitrate solution (triple impregnating mode alternated by intermediate drying at 300–350 °C). The final thermal treatment was performed at 500 °C for 6 h. The content of NiO with respect to the monolith weight was 3.8%.

A monolith catalyst is formed by flat and corrugated gas-tight catalyst strips, which form a porous structure containing large transportation pores-channels (due to corrugation) and small pores (due to gauze porosity). This structure provides favorable conditions for highly intensive catalytic processes such as autothermal reforming of diesel fuels proceeding at high temperatures. The photos of such structured monoliths are shown in Fig. 3. The dimensions of the monolith catalyst are: diameter 55 mm, length 55 mm. All tests were carried out under bench conditions using full-size monolith catalysts. Six catalysts were used in these experiments, and each was operated with several start-ups and shutdowns.

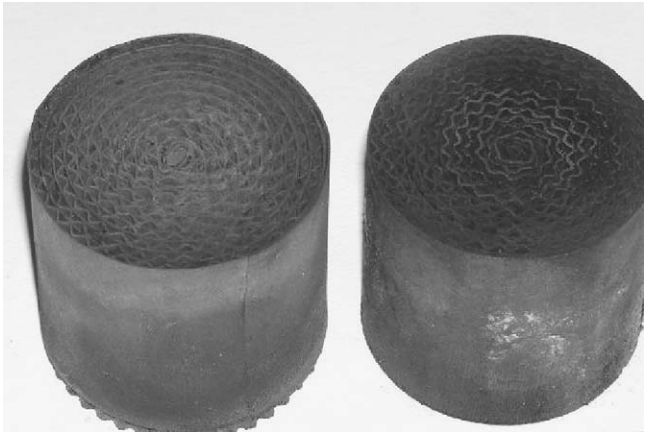

Fig. 3. General view of monolith catalyst.

2.4. Product analysis

The ATR product gases were analyzed using a PEM-2 M gas analyzer with IR detector for CH_4, CO and CO_2 and a dual-column gas chromatograph equipped with sealed column and thermal conductivity detector to determine H_2 and N_2 concentrations.

3. Experimental results and discussion

3.1. Catalyst test operation

At the preliminary stage, the prepared catalysts *A1*, *A2*, *A3*, *A4*, *A5* were subjected to short-term tests in the process of diesel fuel ATR in order to choose the most advanced samples. Resistance of the above catalysts to carbonization and the $H_2/CO>3$ ratio in the reforming products were the selection criteria. Resistance to coke formation was estimated from the catalyst weight changes after bench tests and by appearance. The testes were carried out on one or two consecutively placed monolith catalysts under the following experimental conditions: diesel fuel – 0.044 g/s, O_2/C = 0.5, H_2O/C = 1.5–1.7, T_1 = 350–400 °C. In experiments with catalyst *A1* (Co/Mn/Al_2O_3/gauze), the outlet $H_2/CO>$ ratio was not reached notwithstanding feed variation in a wide concentration range. The concentration of hydrogen in the reforming products of diesel fuel decreased to 23.8%. Besides, the weight of the catalyst during 13 h on stream increases by 11.5 g. This observation most probably associates with the oxidation of the gauze metal in the catalyst support under ATR conditions. In addition, black traces were observed on the catalyst surface.

For the next experiments, catalyst *A1* was replaced by catalyst *A2*. This combination results in acceptable value of H_2/CO ratio, but in lower concentrations of H_2 at the outlet. During 6 h tests the front part of catalyst *A2* endured swelling and weight increase by 6 g. Black traces were also observed.

For the next experiment, catalyst *A3* (Co_2O_3/BaO/MnO_2/fechral gauze) was placed at the reformer inlet and catalyst *A4* (Co_2O_3/BaO/MnO_2/stainless steel) was placed at the reactor outlet. These catalyst pair exhibits stable operation and acceptable H_2/CO ratio. Black traces were also observed. H_2 concentration at the reactor outlet was insufficient.

To increase hydrogen concentration in synthesis gas, catalyst *A4* was replaced by *A5* (rhodium catalyst). In this experiment, the maximum ratio $H_2/CO > 3.5$ and high H_2 concentration in the reforming products were reached; no black traces were observed. Since the test results of this catalyst combination met the technical goals of our work, the catalysts were subjected to further tests. In further experiments, catalyst *A5* was changed by nickel catalyst *A6*. Experiments with catalyst combinations *A3* + *A5* and *A3* + *A6* show similar results. However, in experiments with catalyst combination *A6* + *A3*, considerable carbon deposition (weight increase by 4.1 g) in the channels of catalyst *A6* and a 40 °C temperature increase in the frontal part of the monolith were observed.

Finally, the *A5* + *A3* system was tested. Temperature oscillations up to 40 °C in the frontal part of the first monolith were observed in this experiment. After experiment completion, channels plugging by soot in the first monolith was observed. That is, systems *A5* + *A3* and *A6* + *A3* showed similar hopeless behavior in the test experiments and were rejected from further studies.

Based on the experimental results, catalyst system *A3* + *A5* was considered as the most promising (for detailed data see Table 1).

3.2. Catalyst activity tests

The main criteria for diesel fuel reforming is the maximum yield of H_2 expressed as the molar ratio of the hydrogen contained in the synthesis gas to the carbon contained in the feed – H_2/C. Analysis shows that the maximum possible yield of hydrogen per 1 mol of carbon, H_2/C, is 2.95 for the fuel having H/C = 1.89, based on stoichiometric equation $CH_{1.89} + H_2O = CO_2 + (2 + 1.89/2)H_2$. Such hydrogen yield can be obtained upon steam carbon conversion if shift reactions are not taken into account. For autothermal reforming, hydrogen yield will be lower, because the air oxygen interacts with carbon and thus reduces the effect of the steam reforming reaction.

Since diesel fuel consists of a large number of hydrocarbons with different molecular weights and H_2/C ratios, it is impossible to perform direct thermodynamic analysis of the equilibrium composition of the fuel conversion. For this reason, an approximate thermodynamic analysis of the equilibrium composition was performed for the air-steam reforming of *n*-decane $C_{10}H_{22}$ and benzene C_6H_6 at molar ratio 0.64/0.36. Molecular weight and H_2/C ratio of this mixture are similar to respective characteristics of diesel fuel. The average characteristics of the diesel fuel were determined experimentally and compared to commercial specifications. The H_2/C ratio in the fuel is 1.9. Using this ratio, the molecular weight of the hydrocarbon in the diesel fuel was estimated to be 12 + 1*1.9 = 13.9 g mol, where 12 stands for molecular weight of carbon and 1 stands for molecular weight of hydrogen. Based on the data of chromatographic analysis, estimated average molecular weight of diesel fuel is equal to 140 g mol. Therefore, the average number of the carbon atoms in the diesel molecule is 10. Based on the above estimations, a detailed analysis of the experimental data was carried out (see Table 2). As follows from Table 2, catalyst combination *A3* + *A5* at $O_2/C = 0.5$ and $H_2O/C = 1.6$ can provide the yield of 18 mol of H_2 per 1 mol of diesel fuel. This value exceeds that given in [9]. Note that the concentration of hydrogen in the reaction products is 30%, which approximates the thermodynamically equilibrium value, and the yield of synthesis gas (H_2 + CO) in the experimental runs is 2.88 l/g of diesel fuel at $H_2/CO = 3.5$.

3.3. Durability tests

Durability tests were carried out using full-scale single monolith catalyst *A3* under the following experimental conditions: air – 11.22 l/min, diesel oil – 0.045 g/s, H_2O – 0.1 g/s, T_1 – 308 °C. Fig. 4 presents results of the tests. It is seen that the composition of the reforming products remained unchanged during 70 h. Besides, no carbon deposition and catalyst weight changes were observed.

4. Mathematical model

No data on the kinetics of autothermal reforming of the main diesel fuel components, in particular, *n*-decane, are available in the literature. On the one hand, this is associated with complexity and multi-step character of the chemical reactions occurring during ATR of heavy hydrocarbons (in fact, pyrolysis, cracking, dehydrogenation, partial oxidation, etc. can proceed). On the other hand, the lack of modeling results is explained by a strong effect of the external gas-solid mass transfer on some reaction steps. Here we restrict our theoretical consideration to ATR of individual

Table 2
Experimental data on catalysts combination *A3* + *A5* tests.

Run	Diesel fuel ($g/s \times 10^2$)	Inlet Ratio		Outlet								H_2/CO	$\frac{H_2+CO}{M_{fuel}}$ (l/g)	T^* (°C)	χ (%)
				Measured temperatures (°C)				Composition of reaction products (dry) (% vol.)							
		O/C	S/C	T_1	T_2	T_3	T_4	CH_4	CO_2	CO	H_2				
1	3.197	0.6	1.65	426	969	845	680	2.1	14	7.12	24	3.4	2.09	923	87
2	4.448	0.54	3.19	435	973	850	725	2.5	14	7.97	26	3.3	2.27	820	81
3	4.587	0.52	1.76	344	956	838	654	0.7	14	8.7	30	3.4	2.61	945	95
4	4.587	0.53	1.61	369	932	835	658	2	15	7.71	27	3.5	2.32	967	86
5	4.448	0.54	1.66	408	854	856	695	2	14	7.63	27	3.5	2.30	1026	89
6	4.865	0.49	1.63	357	966	854	667	0.7	14	9.58	32	3.3	2.75	902	98
7	6.672	0.5	1.63	346	911	873	678	0.7	12	11	32	3	2.88	859	97
8	6.533	0.51	1.57	345	907	871	675	0.7	15	8.7	30	3.5	2.65	918	95
9	6.394	0.53	1.52	362	975	897	730	1.9	12	9.9	28	2.8	2.47	975	89
10	6.533	0.51	1.23	395	1010	889	719	1.8	12	12	27	2.3	2.47	1003	87
11	6.394	0.52	2.22	313	893	889	728	1.6	15	8.2	27	3.3	2.29	877	77
12	6.394	0.6	2.17	284	919	936	766	0.9	14	7.6	26	3.4	2.44	985	94
13	9.174	0.52	1.53	244	920	908	726	1.7	11	12	26	2.2	2.46	891	80

$\chi = \left(1 - \frac{H_2^{exp}}{H_2^*}\right)100\%$ – correlation between equilibrium hydrogen fraction (under equilibrium temperature) at the outlet and the experimentally measured value;
T^* – the calculated (adiabatic) thermodynamic equilibrium temperature at the outlet;
H_2^* – the calculated thermodynamic equilibrium hydrogen fraction at the outlet;.
H_2^{exp} – experimentally measured hydrogen fraction at the outlet.

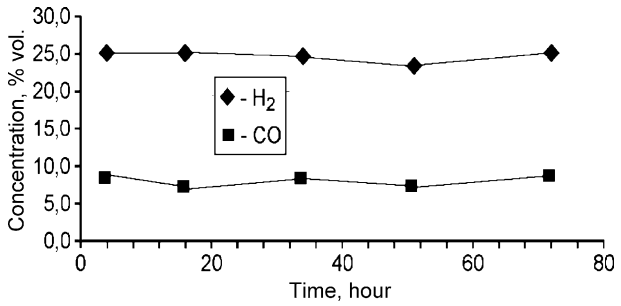

Fig. 4. H_2 and CO outlet fractions in the durability tests of the monolith catalyst *A3*.

hydrocarbon C_nH_{2n+2}. Two reaction routes are assumed to occur simultaneously during ATR:

1) complete oxidation (exothermic route that produces CO_2 and H_2O):

$$C_nH_{2n+2} + \left(\frac{3n+1}{2}\right)O_2 = nCO_2 + (n+1)H_2O, \quad (7)$$

2) steam reforming (endothermic route that produces CO and H_2):

$$C_nH_{2n+2} + n{\cdot}H_2O = n{\cdot}CO + (2n+1)\cdot H_2. \quad (8)$$

Taking into account that there is no available kinetics for *n*-decane combustion, the kinetic expression for isooctane combustion [16] was adopted:

$$W_{ox} = k_{ox}x_{HC}^S x_{O_2}^S, \quad (9)$$

$$k_{ox} = k_{ox}^0 \exp\left(\frac{-E_{ox}}{RT_S}\right). \quad (10)$$

The kinetic rate of steam reforming is assumed to be first order on hydrocarbon and zero order on steam. Such form of steam reforming kinetics is rather common. For example, recent paper [17] reported similar expression both for steam and CO_2 reforming of CH_4:

$$W_{ref} = k_{ref}x_{HC}^S, \quad (11)$$

$$k_{ref} = k_{ref}^0 \exp\left(\frac{-E_{ref}}{RT_S}\right). \quad (12)$$

External mass transfer limitations are taken into account, but internal mass transfer limitations are neglected. The latter assumption is supported by the fact that thickness of the porous catalytic layer was sufficiently small (200–250 μm) for all of *A1–A6* catalysts. The relation between the interphase mass fluxes of oxygen and hydrocarbon and their kinetic rates can be written as:

$$j_{HC} = \beta_{HC}\rho(x_{HC} - x_{HC}^S) = W_{ox} + W_{ref}, \quad (13)$$

$$j_{O_2} = \beta_{O_2}\rho(x_{O_2} - x_{O_2}^S) = W_{ox}\left(\frac{3n+1}{2}\right). \quad (14)$$

If the experimental catalyst temperature at the inlet is about 900–1000 °C, it is reasonable to suggest that the apparent oxidation and reforming rates are controlled by appropriate mass transfer rates:

$$\{k_{ox}, k_{ref}\} >> \{\beta_{HC}\rho, \beta_{O_2}\rho\}.$$

This implies that either one or both gas components HC (hydrocarbon) and/or O_2 exist in relatively small concentrations near the catalyst surface in comparison with respective bulk values:

$$x_{HC}^S << x_{HC} \text{ and/or } x_{O_2}^S << x_{O_2}.$$

The estimations given below confirm that for the inlet gas mixture composition (typical of ATR of diesel fuel) not oxygen but hydrocarbon bulk-surface flux will inevitably control the overall reaction rate. Moreover, this statement remains valid even in the case of complete oxidation (without steam reforming) at the inlet. Actually, at $W_{ref} = 0$, term W_{ox} can be excluded from Eqs. (13)–(14). Then the condition of changing the external mass transfer limiting component between hydrocarbon and oxygen fluxes ($x_{HC}^S \approx 0$, $x_{O_2}^S \approx 0$) can be written as:

$$\psi = \frac{\beta_{O_2}x_{O_2}}{\beta_{HC}x_{HC}((3n+1)/2)} = 1, \quad (15)$$

where ψ can be interpreted as the coefficient of oxygen diffusion excess (calculated for the reaction of complete HC oxidation). For C_nH_{2n+2} with $n = 8$–16, the ratio for the mass transfer/diffusion coefficients between *O2/HC* (in air at 350 °C) occupies the interval:

$$\frac{\beta_{O_2}}{\beta_{HC}} = \frac{D_{O_2}}{D_{HC}} = 3.6 - 5.7.$$

$$\text{More strictly, for n-decane } (C_{10}H_{22}): \frac{\beta_{O_2}}{\beta_{HC}} = \frac{D_{O_2}}{D_{HC}} = 4.4. \quad (16)$$

In our experiments on diesel fuel ATR, we used the inlet ratio $O_2/C = 0.5$–0.7, i.e. for *n*-decane ($n = 10$), it will be:

$$\frac{x_{O_2}}{x_{HC}} = n\left(\frac{O_2}{C}\right) = 5 - 7. \quad (17)$$

Inserting terms (16), (17) into (15), we get the desired estimation for ψ :

$$1.4 < \psi < 2.$$

This important estimation indicates that for our experimental conditions, the ATR process (at least not very far from the catalyst bed inlet) is controlled by bulk-surface flux of hydrocarbons (rather than oxygen), because the (value, which is defined by expression (15), is larger than 1. If we take into account the parallel reaction step of steam reforming, the value of oxygen excess near the catalyst surface will only increase ((will increase). Limiting of the ATR reaction rate by hydrocarbons external mass transfer implies that $x_{HC}^S << x_{HC}$ or in the ideal case $x_{HC}^S \to 0$. As a result, Eq. (13) can be reduced to the form:

$$j_{HC} = \beta_{HC}\rho x_{HC} = W_{ox} + W_{ref}.$$

So, one can see that the total hydrocarbon flux is "divided" on the catalyst surface in two different parts: one part undergoes complete oxidation (7), the other is engaged in steam reforming (8). The key theoretical question arises here: how to divide total flux into two parts and is this division kinetically controlled? Below we suggest the original modeling approach for determination of apparent rates of these two parallel reaction steps. Firstly, it is convenient to define partial fractions for oxidation and reforming routes ($_{ox}$, ($_{ref}$ as

$$W_{ox} = \varphi_{ox}j_{HC}, \quad W_{ref} = \varphi_{ref}j_{HC}, \quad \varphi_{ox} + j_{ref} = 1. \quad (18)$$

Taking into account (9)–(12), the ratio between reaction rates may be expressed as:

$$\frac{W_{ref}}{W_{ox}} = \frac{k_{ref}x_{HC}^S}{k_{ox}x_{HC}^S x_{O_2}^S} = \frac{k_{ref}}{k_{ox}x_{O_2}^S} = \frac{(k_{ref}^0/k_{ox}^0)\exp[-(E_{ref} - E_{ox})/RT_S]}{x_{O_2}^S} = \frac{k_0\exp(-E/RT_S)}{x_{O_2}^S} = \frac{k}{x_{O_2}^S}, \quad (19)$$

where $k_0 = k^0_{ref}/k^0_{ox}$, $E = E_{ref} - E_{ox}$, $k = k_0 \exp(-E/RT_S)$.

On the other hand, according to (18):

$$\frac{W_{ref}}{W_{ox}} = \frac{\varphi_{ref}}{\varphi_{ox}} = \frac{1-\varphi_{ox}}{\varphi_{ox}}. \quad (20)$$

Comparing the right sides of (19) and (20), we get expressions for the fraction of oxidation and reforming reaction step:

$$\varphi_{ox} = \frac{x^S_{O_2}}{x^S_{O_2}+k} = \frac{x^S_{O_2}}{x^S_{O_2}+k_0\exp(-E/RT_S)}, \quad \varphi_{ref} = 1-\varphi_{ox}. \quad (21)$$

It remains only to determine the value of oxygen concentration near catalytic surface $x^S_{O_2}$ in Eq. (21). For this purpose, the below expression for W_{ox}, which is obtained from (18), (21), is then introduced into Eq. (14):

$$W_{ox} = \varphi_{ox} j_{HC} = \left(\frac{x^S_{O_2}}{x^S_{O_2}+k}\right) j_{HC}.$$

Finally, we get the following equation:

$$\beta_{O_2}\rho(x_{O_2} - x^S_{O_2}) = \left(\frac{x^S_{O_2}}{x^S_{O_2}+k}\right) j_{HC}\left(\frac{3n+1}{2}\right). \quad (22)$$

Eq. (22) is easily reduced to a quadratic equation with unknown $x^S_{O_2}$. Elementary analysis of Eq. (22) shows that under condition $kx_{O_2} > 0$ (which is always true) only one positive root of this equation exists, which has physical meaning of oxygen concentration near the catalytic surface. Thus, the mathematical description of reaction rates in the considered reaction network becomes complete.

For description of transfer processes along the catalyst bed, we considered a one-dimensional stationary heterogeneous model of an adiabatic plug-flow reactor. Axial heat dispersion effect is neglected in the mathematical model. The initial reason for this simplification was: two experimental monoliths were stacked so that the distance of 1–2 mm was kept between them. The following results of modeling and comparison with the experimental temperature measurements completely justified this assumption.

$$\begin{aligned}
G\frac{dy_{HC}}{d\ell} &= -(W_{ox}+W_{ref})Sm_{HC},\\
G\frac{dy_{O_2}}{d\ell} &= -W_{ox}\left(\frac{3n+1}{2}\right)Sm_{O_2},\\
G\frac{dy_{H_2O}}{d\ell} &= (W_{ox}(n+1) - W_{ref}n)Sm_{H_2O},\\
G\frac{dy_{CO}}{d\ell} &= (W_{ref} - W_{sh})nSm_{CO},\\
G\frac{dy_{CO_2}}{d\ell} &= (W_{ox})nSm_{CO_2},\\
G\frac{dy_{H_2}}{d\ell} &= (W_{ref}(2n+1))Sm_{H_2},\\
c_pG\frac{dT_g}{d\ell} &= \alpha S(T_S - T_G),\\
W_{ox}\Delta H_{ox} - W_{ref}\Delta H_{ref} &= \alpha(T_S - T_g).
\end{aligned} \quad (23)$$

Coefficients of heat-mass transfer:

$$\alpha = \frac{Nu\lambda}{\alpha}, \quad \beta_{HC} = \frac{D_{HC}Sh}{d}, \quad \beta_{O_2} = \frac{D_{O_2}Sh}{d}.$$

Thus, we have determined all the dependencies required for calculations using a mathematical model (18)–(23). It is worthy to note that the developed modeling approach does not require the direct knowledge of rate constants for oxidation (10) and reforming (12) reaction routes. It is sufficient only to specify a ratio between these rate constants, more exactly, a ratio between its factors $k_0 = k^0_{ref}/k^0_{ox}$ and difference in activation energies of both reaction routes $E = E_{ref} - E_{ox}$.

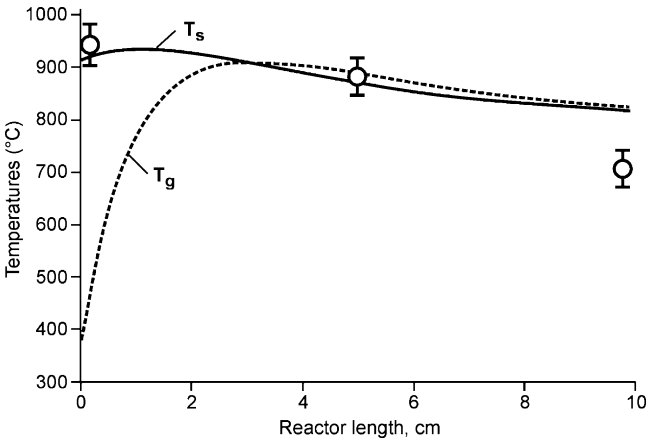

Fig. 5. Experimental and calculated data on temperature distribution along the catalyst bed under autothermal diesel fuel reforming. Inlet conditions: T_g = 346 °C; Q_{air} = 15.4 l/min; Q_{H2O} = 504 g/h; Q_{HC} = 240 g/h, which corresponds to H_2O/C = 1.67, O_2/C = 0.5.

5. Results of modeling

Figs. 5–8 present the calculated and experimental data (scattering is shown as vertical line segments) for a typical operation mode of the reactor. The experimental conditions at the inlet were: gas mixture temperature 346 °C; air flow rate 15.4 l/min; water flow rate 504 g/h; diesel fuel flow rate 240 g/h. Calculations were made for *n*-decane as a representative of diesel fuel, the inlet (molar) composition of the gas mixture was: nitrogen 45.5%, steam 40%, oxygen 12.1%, *n*-decane 2.4%.

Fig. 5 illustrates the temperature profile. The calculated axial temperature gradient for solid phase is rather small (less than hundred degrees per 10 cm). So, the additional account for axial heat conductivity in the model would have no significant influence on steady-state regime of the reactor (but not for dynamic regime, i.e. start-up). The gas-solid temperature difference at the inlet is determined by the interplay between oxidation and steam reforming reactions. There is no available data in the literature concerning activation energies of oxidation and steam reforming of *n*-decane, but for isooctane these values are [16]: E_{ref} = 240 kJ/mol, $E_{ox} \approx$ 160 kJ/mol. Our approach needs only the knowledge of the difference between them. So, in our case

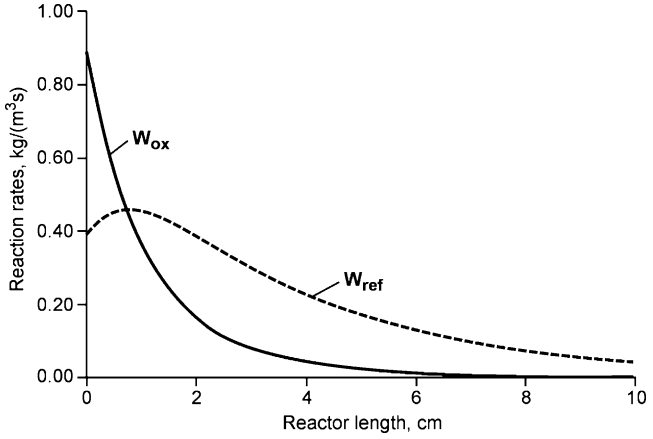

Fig. 6. Distribution of apparent reaction rates along the catalyst bed under autothermal diesel fuel reforming. The conditions are identical to those in Fig. 5.

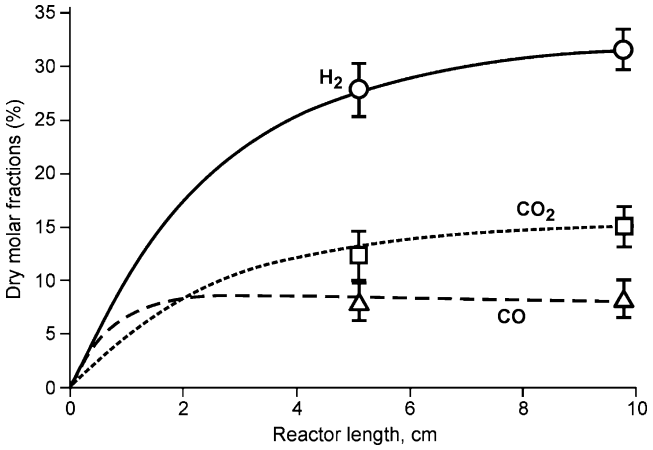

Fig. 7. Experimental and calculated distributions of "dry" molar fractions of reaction products along the catalyst bed length under autothermal diesel fuel reforming. The conditions are identical to those in Fig. 5.

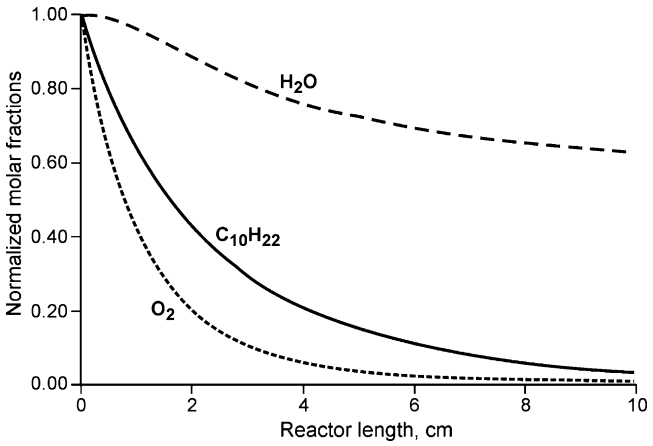

Fig. 8. Distribution of reagent mole concentrations normalized to their inlet values (*n*-decane, oxygen, water) along the catalyst bed under autothermal diesel fuel reforming. The conditions are identical to those in Fig. 5.

we take $E = E_{ref} - E_{ox} = 80$ kJ/mol. Selecting an appropriate value of preexponential factor (19) $k_0 = 102$ (while parameter E is already fixed), we can get an excellent matching of the experimental and modeled values of the inlet catalyst temperature. Note that the molar fraction of oxygen near the catalyst surface is 6.3% (the bulk value at the inlet is 12%). The rate of oxidation at the inlet is twice larger than the rate of steam reforming. This is directly shown in Fig. 6, which exhibits the distribution of both reaction rates along the catalyst bed. At the inlet, the rate of oxidation exceeds that of reforming, which results in slight catalyst temperature maximum T_S (Fig. 5). In the course of rapid oxygen consumption, oxidation rate W_{ox} drops along the reactor, whereas the rate of steam reforming W_{ref} remains rather high. This explains an interval of the monotonous temperature decrease with an asymptotic approximation to the equilibrium value. A noticeable deviation of experimental temperature down from the calculated value at the outlet can be explained by heat losses. Important, the calculations performed at activation energies varying within the interval $0 < E < 180$ kJ/mol (with simultaneous appropriate selection of k_0 so as to match the experimental inlet catalyst temperature) exhibited a weak sensitivity of the model solution to this parameter. For example, at $E = 0$ (i.e. equal activation energies of oxidation and reforming), the calculated temperature maximum increases by 50 °C if compared to Fig. 5. Fig. 7 shows a comparison of the calculated profiles of "dry" molar fractions of H_2, CO, CO_2 and the experimental data collected after the first monolith (5 cm) and after the second one, i.e. at the reactor outlet (10 cm). Fig. 8 presents normalized (by their inlet values) molar fractions of reagents: *n*-decane, oxygen and steam. High excess of steam in the mixture over the entire reactor and the rapid consumption of oxygen (in comparison to hydrocarbon) are clearly seen.

6. Discussion and conclusion

Six catalyst composites for the diesel fuel ATR have been developed based on the reinforced gauze support. The developed catalysts were tested during short-term (several hours) and long-term (70 h) tests. As follows from the experiments, catalyst system *A3* + *A5* is the most promising for autothermal reforming of diesel fuels. Based on the experimental results, the optimum operation conditions were specified: $O_2/C = 0.5–0.6$, $H_2O/C = 1.5–1.7$, contact time 0.3–0.4 s, temperature of mixture at the reactor inlet 300–400 °C. At these conditions, the reaction products contain: $H_2 = 32\%$, $CH_4 = 1\%$, $CO_2 = 12\%$, $CO = 11\%$, $N_2 = 44\%$. Yield of $H_2 + CO$ is 2.88 l/g (fuel), the hydrogen yield is 18 mol/mol (fuel), $H_2/CO = 3.5$ in the reaction products.

The mathematical model of diesel fuel ATR in the structured catalyst bed was developed. The experimental and modeling data were compared for one process regime: S/C = 1.67, O/C = 1. The model is based on the assumption that two reaction routes exist under the ATR conditions: (1) complete oxidation of hydrocarbon, (2) steam reforming of hydrocarbon. Both reaction routes proceed simultaneously and start just at the catalyst entrance. The process is controlled by the gas–solid interphase mass transfer of hydrocarbon. Note that the ratio between the above competing steps, i.e. division of the diffusion hydrocarbon flux between them, is determined by the ratio of kinetic constants of these reaction routes and by near the catalyst surface oxygen concentration.

An evident conclusion is that a catalyst operating well during this process should also exhibit high activity in the steam reforming even in the presence of oxygen. This factor is important for preventing catalyst overheating (the so-called hot spot) in the inlet catalyst bed zone. More precisely, the catalyst should provide some optimal ratio between the exothermic and endothermic reaction steps (under constant diffusion flux of hydrocarbons to the surface). In the suggested model, this ratio is characterized by two parameters: $E = E_{ref} - E_{ox}$, $k_0 = k_{ref}^0/k_{ox}^0$. If a catalyst is insufficiently active in the reaction of complete oxidation, its "ignition" might require too high temperature of the inlet gas mixture (which may result in the thermal cracking). If a catalyst is insufficiently active in the reaction of steam reforming in the presence of oxygen, a danger of catalyst overheating in the oxidation zone inevitably appears. Based on the above concepts, one can make conclusions concerning the potential of the suggested catalysts.

Without question, the fact that we incorporate in the model only three reaction routes (oxidation, steam reforming, shift) is an idealization. This is, in particular, confirmed by methane residuals at the reactor outlet. Nevertheless, to our mind, the first step made in the field of connection between experiment and modeling of ATR diesel reforming reactors appeared promising.

Acknowledgements

The authors gratefully acknowledge the financial support of this work from International Science and Technology Center (ISTC) under Project 3389.

References

[1] M. Krumpelt, T.R. Krause, J.D. Carter, J.P. Kopasz, S. Ahmed, Catal. Today 77 (2002) 3.

[2] T. Krause, J.M. Mawdsley, C. Rossignol, J. Kopasz, D. Applegate, M. Ferrandon, J.D. Carter, M. Krumpelt, in ANL FY Progress Report "Hydrogen, Fuel Cells, and Infrastructure Technologies", 2002.
[3] J.M. Mawdsley, M. Ferrandon, C. Rossignol, J. Ralph, L. Miller, J. Kopasz, T. Krause, in ANL FY Progress Report "Hydrogen, Fuel Cells, and Infrastructure Technologies", 2003.
[4] D.A. Berry, D. Shekhawat, T.H. Gardner, in DOE National Energy Technology Laboratory FY Report "Hydrogen, Fuel Cells, and Infrastructure Technologies", 2003.
[5] C. Pereira, J-M Bae, S. Ahmed, M. Krumpelt, Report under Contract W-31-109-ENG-38, 2000.
[6] J. Pasel, J. Meissner, Z. Pors, C. Palm, P. Cremer, R. Peters, D. Stolten, Fuel Cells 4 (2004) 225.
[7] J.P. Kopasz, D.J. Liu, S. Lottes, R. Ahluwalia, V. Novick, S. Ahmed, in ANL FY Progress Report "Hydrogen, Fuel Cells, and Infrastructure Technologies", 2003.
[8] D.A. Berry, D. Shekhawat, T.H. Gardner, W. Rogers, in DOE National Energy Technology Laboratory FY Report "Hydrogen, Fuel Cells, and Infrastructure Technologies", 2002.
[9] T. Krause, M. Ferrandon, J. Mawdsley, J. Ralph, in ANL FY Progress Report "DOE Hydrogen Program", 2004.
[10] S. Roychoudhury, M. Castaldi, M. Lyubovsky, R. LaPierre, S. Ahmed, J. Power Sources 152 (2005) 75.
[11] S. Roychoudhury, M. Lyubovsky, D. Walsh, D. Chu, E. Kallio, J. Power Sources 160 (2006) 510.
[12] J.J. Krummenacher, K.N. West, L.D. Schmidt, J. Catal 215 (2003) 332.
[13] R. Subramanian, G.J. Panuccio, J.J. Krummenacher, I.C. Lee, L.D. Schmidt, Chem. Eng. Sci. 59 (2004) 5501.
[14] B.J. Dreyer, I.C. Lee, J.J. Krummenacher, L.D. Schmidt, Appl. Catal. A: Gen. 307 (2006) 184.
[15] V.A. Kirillov, A.S. Bobrin, N.A. Kuzin, V.A. Kuzmin, A.B. Shigarov, V.B. Skomorokhov, E.I. Smirnov, V.A. Sobyanin, Ind. Eng. Chem. Res. 43 (2004) 4721.
[16] G.A. Petrachi, G. Negro, S. Specchia, G. Saracco, P.L. Maffettone, V. Specchia, Ind. Eng. Chem. Res. 44 (2005) 9422.
[17] J. Wei, E. Iglesia, J. Catal. 224 (2004) 370.